

Cite this: *Mater. Adv.*, 2020,  
1, 326Received 5th April 2020,  
Accepted 9th May 2020

DOI: 10.1039/d0ma00168f

rsc.li/materials-advances

# The surfactant-free bottom-up synthesis of ultrathin MOF nanosheets for the oxidation of isoeugenol to vanillin†

Vijayan Srinivasapriyan  <sup>ab</sup>

The direct synthesis of ultrathin MOF nanosheets is extremely challenging. Plenty of methods have been developed for the fabrication of MOF nanosheets, but these nanosheets suffer from structural deterioration, aggregation, morphological fragmentation, and low yields. Therefore, the direct synthesis of MOF nanosheets is more desirable, but this relies on our ability to easily and controllably synthesize them, which remains a challenging task. Herein, we report the direct bottom-up synthesis of MOF nanosheets comprising of assemblies of single layers, producing high crystallinity, surfactant-free low-cost MOF nanosheets with high yield.

Metal organic frameworks (MOFs) constitute one of the most fascinating subjects in the fields of chemistry and material science.<sup>1–10</sup> They are made of metal ions or clusters with organic molecules, and their high surface areas, ultrahigh porosity, and tunable structures and functions provide lots of application in the field of catalysis.<sup>11–15</sup> MOF nanosheets constitute a new member of the 2D nanomaterial family and a subject of fundamental studies and quite interesting applications due to their highly exposed active sites.<sup>16–21</sup> More importantly, like other 2D materials, their ultrathin nature and large lateral sizes also make them promising for surface-active applications. Direct synthesis of an ultrathin MOF nanosheet is extremely challenging, and achieving such an MOF nanosheet in high yield and displaying high crystallinity is extremely difficult. MOF nanosheets have been fabricated using two approaches: the top-down approach involves delamination of layered MOF precursors *via* methods such as sonication and chemical intercalation, but suffers from low yield and structural deterioration and morphological fragmentation during exfoliation;<sup>22,23</sup> the direct bottom-up synthesis of MOF nanosheets is more desirable but relies on our ability to direct crystal growth to form high-aspect-ratio nanosheets

at a reasonable yield. Apart from a few recent reports, only two series of MOFs have to date been directly synthesized as ultrathin nanosheets dispersible in solvents: Rodenas *et al.* reported a three-layer synthesis method for M-BDC (M = Cu, Co, BDC = 1,4-benzenedicarboxylate) nanosheets by modulating the growth kinetics of MOF crystals, but this approach often displays low yields and does not offer good control over the morphology of the nanosheets; later Zhao *et al.* introduced a PVP as a surfactant in the synthesis of M-TCPP (M = Zn, Cu, Cd, Co, TCPP = tetrakis(4-carboxyphenyl)porphyrin) nanosheets, but the PVP surfactant would probably need to be removed to utilize properly the exposed active surfaces of the nanosheets. Here we report the direct synthesis of highly crystalline nanosheets comprising assemblies of a single layer. The direct synthesis of ultrathin cobalt MOF Co(Hoba)<sub>2</sub>·2H<sub>2</sub>O (Hoba = 4,4-oxybis(benzoic acid)) was originally reported in the form of bulk materials.<sup>24</sup> With the direct synthesis method reported here, ultrathin surfactant-free cobalt nanosheets were produced at low cost and in high yield, and showed neither morphological fragmentation nor deterioration nor aggregation.

The fabrication of cobalt MOF nanosheets was accomplished using the direct bottom-up method. First, we optimized the reaction conditions for the fabrication by screening several parameters such as solvent, temperature, reaction time, relative molar amount of reactant, and whether base was present. In this optimized fabrication of the ultrathin cobalt nanosheets, Co(NO<sub>3</sub>)<sub>2</sub>·6H<sub>2</sub>O (0.4 mmol) and Hoba (0.8 mmol) were mixed in 5 mL of distilled water, and 20 μL of TEA were added into the solution to adjust the pH value to ~7.00. And then the pH-adjusted solution was kept in a 20 mL Teflon-lined stainless-steel autoclave heated at 120 °C for 12 h, followed by being cooled to room temperature. The resulting mixture was centrifuged and washed with ethanol several times and dried at 60 °C in a vacuum oven for 12 h. Finally a pink-colored MOF with a 60% yield was collected.

Fig. 1 displays the results indicating the successful fabrication of ultrathin cobalt MOF nanosheets. The acquired SEM and TEM images showed the layered structure of the cobalt MOF nanosheets.

<sup>a</sup> CAS Key Laboratory of Nanosystem and Hierarchical Fabrication, CAS Center for Excellence in Nanoscience, National Center for Nanoscience and Technology, Beijing 100190, China. E-mail: vsripriyan@live.in

<sup>b</sup> University of Chinese Academy of Sciences, Beijing 100049, China

Electronic supplementary information (ESI) available. See DOI: 10.1039/d0ma00168f



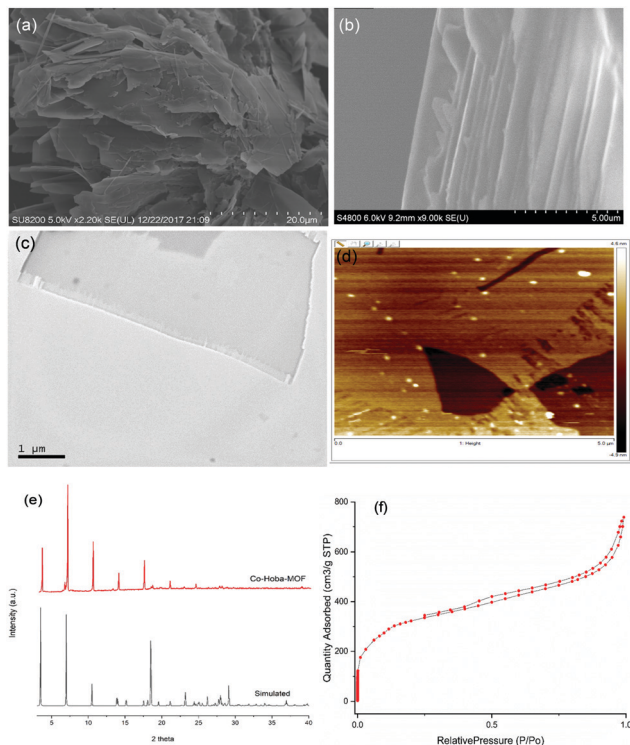


**Fig. 1** (a and b) SEM images, (c) a TEM image, (d) an AFM image, (e) PXRD results, and (f)  $N_2$  adsorption–desorption isotherms of the synthesized Co-Hoba MOF.

In order to further study the crystal structure of nanosheets, X-ray diffraction (XRD) measurements were taken. The powder X-ray diffraction pattern confirmed that the synthesized MOF nanosheets were highly crystalline. An atomic force microscopy (AFM) image revealed an average sheet thickness of  $\sim 10$  nm. The Brunauer–Emmett–Teller (BET) surface area obtained was  $1189\text{ m}^2\text{ g}^{-1}$ .

The fabrication of nickel MOF nanosheets was also accomplished using the direct bottom-up method. Here, too, we first we optimized the reaction conditions for the fabrication by screening several parameters such as solvent, temperature, reaction time, relative molar amount of reactant, and whether base was present. In this optimized fabrication of the ultrathin nickel nanosheets,  $\text{Ni}(\text{NO}_3)_2 \cdot 6\text{H}_2\text{O}$  (0.4 mmol) and Hoba (0.8 mmol) were mixed in 5 mL of distilled water, and 20  $\mu\text{L}$  of TEA were added into the solution to adjust the pH value to  $\sim 7.00$ . The pH-adjusted solution was kept in a 20 mL Teflon-lined stainless-steel autoclave heated at  $120^\circ\text{C}$  for 12 h, followed by being cooled to room temperature. The resulting mixture was centrifuged and washed with ethanol several times and dried at  $60^\circ\text{C}$  for 12 h. Finally, the greenish-colored MOF was collected with a 56% yield.

Fig. 2 displays the results indicating the successful fabrication of ultrathin nickel MOF nanosheets. The acquired SEM and TEM images showed the layered structure of the nickel MOF nanosheets. In order to further study the crystal structure of the nanosheets, X-ray diffraction (XRD) measurements were taken. The powder X-ray diffraction pattern confirmed that the

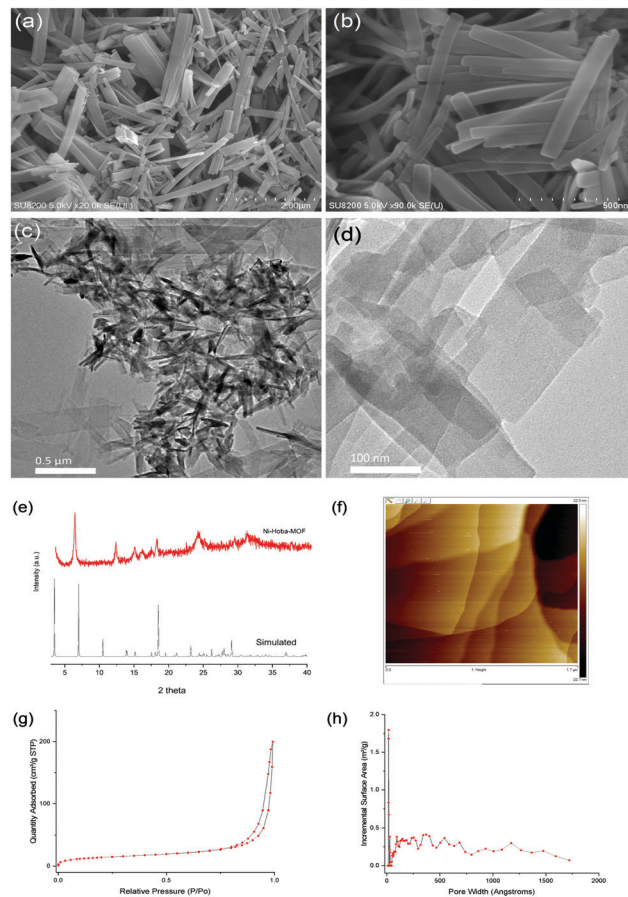


**Fig. 2** (a and b) SEM images, (c and d) TEM images, (e) PXRD results, (f) an AFM image, (g)  $N_2$  adsorption–desorption isotherms, and (h) the pore size distribution of the synthesized Ni-Hoba MOF.

synthesized MOF nanosheets were highly crystalline. An AFM image revealed an average sheet thickness of  $\sim 15$  nm. The Brunauer–Emmett–Teller (BET) surface area obtained was  $52\text{ m}^2\text{ g}^{-1}$ .

Vanillin is one of the most commonly used natural products.<sup>25</sup> It is a vital chemical in the aroma industry, and is abundantly used in the pharmaceutical, food, cosmetic, and chemical industries. Therefore, lots of research has been aimed at improving its production. The chemical synthesis of vanillin is well-established in large-scale production from lignin-derived feedstocks. These classical synthetic routes, however, are not environmentally friendly and the vanillin produced using these methods is considered to be of lower quality because it does not contain some trace components that contribute to the natural vanilla flavor. These trace compounds are easily derived from lignin and have a structural unit common with that of vanillin, being potentially useful for vanillin production *via* simple oxidation pathways. Another problem with the classical synthetic routes is their slow reaction rates, unsuitable for commercial production. As a result, chemical oxidation pathways have also been followed in order to achieve faster reactions and better selectivity of vanillin. And lignin-derived monomers (such as eugenol, isoeugenol, ferulic acid, *etc.*) have been used in the past few years. However, replacing the existing processes with a selective and

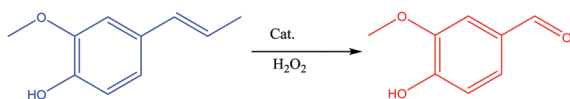


Table 1 Synthesis of vanillin with various catalysts under standard conditions<sup>a</sup>

| No. | Catalyst | Conversion (%) | Selectivity (%) |
|-----|----------|----------------|-----------------|
| 1   | Co-Hoba  | 18             | 90              |
| 2   | Ni-Hoba  | 23             | 92              |
| 3   | Cu-Hoba  | 10             | 82              |

<sup>a</sup> Reaction conditions: 0.5 mL of isoeugenol, cat: 20 mg, H<sub>2</sub>O<sub>2</sub> – 2 mL, rt, 24 h.

efficient production of vanillin from these feedstocks remains an issue (Table 1).



Specifically, we first optimized the reaction conditions for the fabrication by screening several parameters such as the oxidant, solvent, and catalyst. From the screening tests, we concluded that the synthesis of vanillin from isoeugenol would best occur with H<sub>2</sub>O<sub>2</sub> as an oxidant, acetonitrile as a solvent, and Ni-Hoba MOF as a catalyst.

In summary, we have developed a facile direct bottom-up method to synthesize MOF nanosheet assemblies of single layers, and applied the method to Co and Ni MOFs. The two products were surfactant-free and showed neither morphological fragmentation nor deterioration nor aggregation. Furthermore, the developed method is simple and efficient, and can achieve the product in high yield. And we expect the method to find use in synthesizing other ultrathin MOF nanosheets, which in turn might have promising applications in the synthesis of vanillin. In such a synthesis of vanillin, we achieved moderate conversion with good selectivity.

## Conflicts of interest

There are no conflicts to declare.

## Acknowledgements

The authors gratefully acknowledge financial support from the CAS – TWAS president's fellowship.

## References

- H. Furukawa, K. E. Cordova, M. O'Keeffe and O. M. Yaghi, *Science*, 2013, **341**, 1230444.
- N. S. Bobbitt, M. L. Mendonca, A. J. Howarth, T. Islamoglu, J. T. Hupp, O. K. Farha and R. Q. Snurr, *Chem. Soc. Rev.*, 2017, **46**, 3357–3385.
- P. Ji, J. B. Solomon, Z. Lin, A. Johnson, R. F. Jordan and W. Lin, *J. Am. Chem. Soc.*, 2017, **139**, 11325–11328.
- A. Dhakshinamoorthy, A. M. Asiri and H. Garcia, *Chem. Soc. Rev.*, 2015, **44**, 1922–1947.
- A. Corma, H. Garcia and F. Llabrés i Xamena, *Chem. Rev.*, 2010, **110**, 4606–4655.
- H.-C. Zhou, J. R. Long and O. M. Yaghi, *Chem. Rev.*, 2012, **112**(2), 673–674.
- S. Kitagawa, *Chem. Soc. Rev.*, 2014, **43**, 5415–5418.
- H. Zhang, G. Liu, L. Shi, H. Liu, T. Wang and J. Ye, *Nano Energy*, 2016, **22**, 149–168.
- H. Zhang, J. Nai, L. Yu and X. W. D. Lou, *Joule*, 2017, **1**, 77–107.
- V. Srinivasapriyan, *Nanoscale Adv.*, 2019, **1**, 3379–3382.
- M. Zhao, Y. Wang, Q. Ma, Y. Huang, X. Zhang, J. Ping, Z. Zhang, Q. Lu, Y. Yu and H. Xu, *Adv. Mater.*, 2015, **27**, 7372–7378.
- X. Wang, C. Chi, K. Zhang, Y. Qian, K. M. Gupta, Z. Kang, J. Jiang and D. Zhao, *Nat. Commun.*, 2017, **8**, 14460.
- T. Rodenas, I. Luz, G. Prieto, B. Seoane, H. Miro, A. Corma, F. Kapteijn, F. Llabrés i Xamena and J. Gascon, *Nat. Mater.*, 2015, **14**, 48.
- M. Zhao, Y. Huang, Y. Peng, Z. Huang, Q. Ma and H. Zhang, *Chem. Soc. Rev.*, 2018, **47**, 6267–6295.
- A. Dhakshinamoorthy, A. M. Asiri and H. Garcia, *Adv. Mater.*, 2019, **31**, 1900617.
- D. Sheberla, J. C. Bachman, J. S. Elias, C.-J. Sun, Y. Shao-Horn and M. Dincă, *Nat. Mater.*, 2017, **16**, 220.
- P.-Q. Liao, N.-Y. Huang, W.-X. Zhang, J.-P. Zhang and X.-M. Chen, *Science*, 2017, **356**, 1193–1196.
- G. Xu, H. Zhang, J. Wei, H.-X. Zhang, X. Wu, Y. Li, C. Li, J. Zhang and J. Ye, *ACS Nano*, 2018, **12**, 5333–5340.
- W. Zheng, C.-S. Tsang, L. Y. S. Lee and K.-Y. Wong, *Mater. Today Chem.*, 2019, **12**, 34–60.
- J. Duan, Y. Li, Y. Pan, N. Behera and W. Jin, *Coord. Chem. Rev.*, 2019, **395**, 25–45.
- H. Li, J. Hou, T. D. Bennett, J. Liu and Y. Zhang, *J. Mater. Chem. A*, 2019, **7**, 5811–5818.
- J. Zhang, A. V. Biradar, S. Pramanik, T. J. Emge, T. Asefa and J. Li, *Chem. Commun.*, 2012, **48**, 6541–6543.
- S. Wu, L. Qin, K. Zhang, Z. Xin and S. Zhao, *RSC Adv.*, 2019, **9**, 9386–9391.
- J. Lee, O. K. Farha, J. Roberts, K. A. Scheidt, S. T. Nguyen and J. T. Hupp, *Chem. Soc. Rev.*, 2009, **38**, 1450–1459.
- D. Hua, C. Ma, S. Lin, L. Song, Z. Deng, Z. Maomy, Z. Zhang, B. Yu and P. Xu, *J. Biotechnol.*, 2007, **130**, 463–470.

